Forecasting axionic isocurvature detectability in Euclid and MegaMapper using EFTofLSS

[2306.09456]

Work with **Sai Tadepalli**

Daniel J. H. Chung

THE UNIVERSITY of WISCONSIN MADISON

and Prof Moritz Muenchmeyer

Generic class of models for a blue isocurvature spectrum

Consider a QCD axion sector whose PQ symmetry breaking direction is lifted by gravity mediated mass scale of O(H) during inflation.

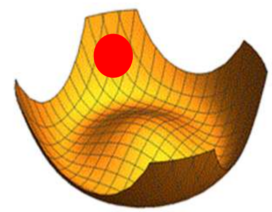

Suppose the radial field is **out of equilibrium**:

Goldstone theorem is violated:

$$\mathcal{L} \ni \frac{\partial_0^2 S}{2S} A^2 + \ldots$$

where

$$\Phi = \frac{S}{\sqrt{2}} e^{iA/S}$$

Axion isocurvature gets a blue tilt

$$n_{\rm iso} - 1 = 3 - 3\sqrt{1 - \frac{4m_A^2}{9H^2}}$$

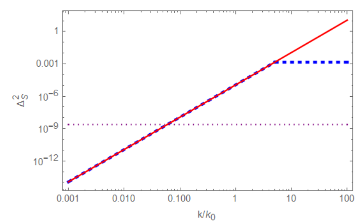

$$k^3 \widetilde{\langle AA \rangle'} \sim k^{n_{\rm iso}-1}$$

$$\frac{k^3}{2\pi^2} P_{S_{cdm}}(k) = A_{\rm iso}(k_{\rm p}) \left(\frac{k}{k_{\rm p}}\right)^{n_{\rm iso}-1}$$

Horizon exit → background field dynamics govern the quantum k dependence

Somewhat natural in SUSY models [Kasuya, Kawasaki 0904.3800]

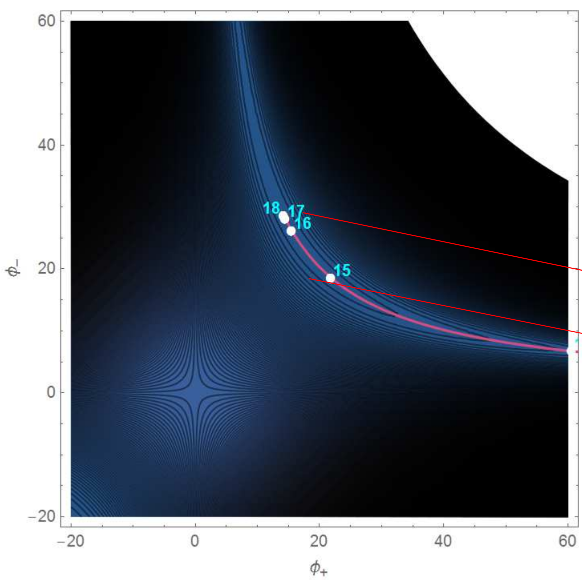

e.g.

$$W = h(\Phi_+ \Phi_- - F_a^2)\Phi_0$$

$$V_K = c_+ H^2 |\Phi_+|^2 + c_- H^2 |\Phi_-|^2 + c_0 H^2 |\Phi_0|^2$$

$$n_{\rm iso} = 3 - \sqrt{9 - 4\frac{m_A^2}{H^2}}$$

Axion isocurvature

1610.04284

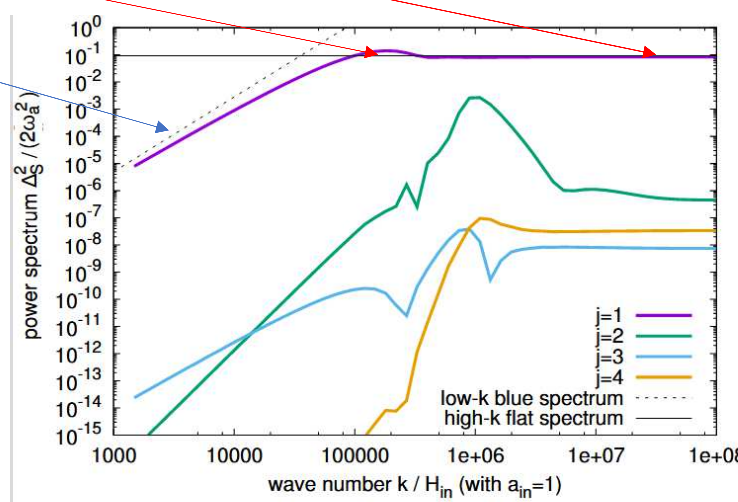

There can also be resonant oscillatory phenomena for **heavy** radial masses:

[2110.02272]

$$\phi_+(T) \sim \exp\left(\left[-1+\sqrt{1-\tfrac{4}{9}\tfrac{m^2_{\text{descent}}}{H^2}}\right]\tfrac{3}{2}T\right)$$
$$\phi_-(T) \sim \frac{F^2}{\phi_+}$$

$$m^2_{\text{descent}} > \frac{9}{4}H^2$$

$$\phi_+(T) \sim \exp\left(-\frac{3}{2}T\right)\cos\left(\sqrt{\frac{m^2_{\text{descent}}}{H^2}-\frac{9}{4}}T-\varphi\right)$$
$$\phi_-(T) \sim \frac{F^2}{\phi_+}$$

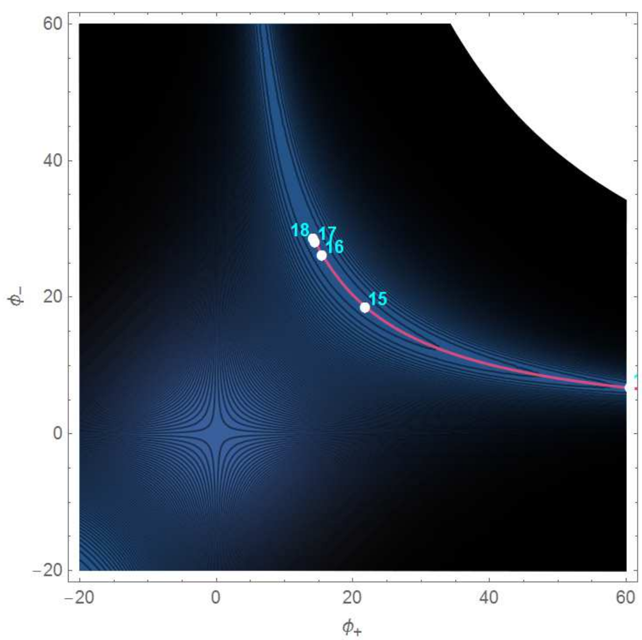

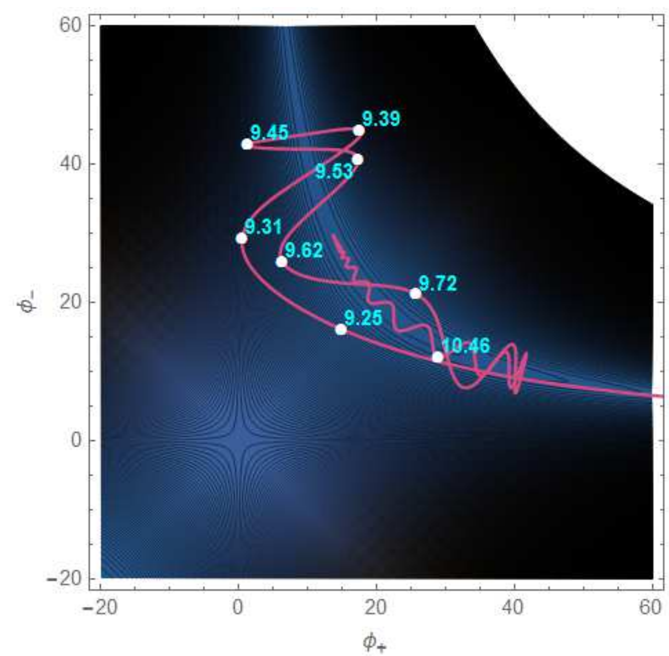

[2110.02272] An interesting example plot of the analytic result:

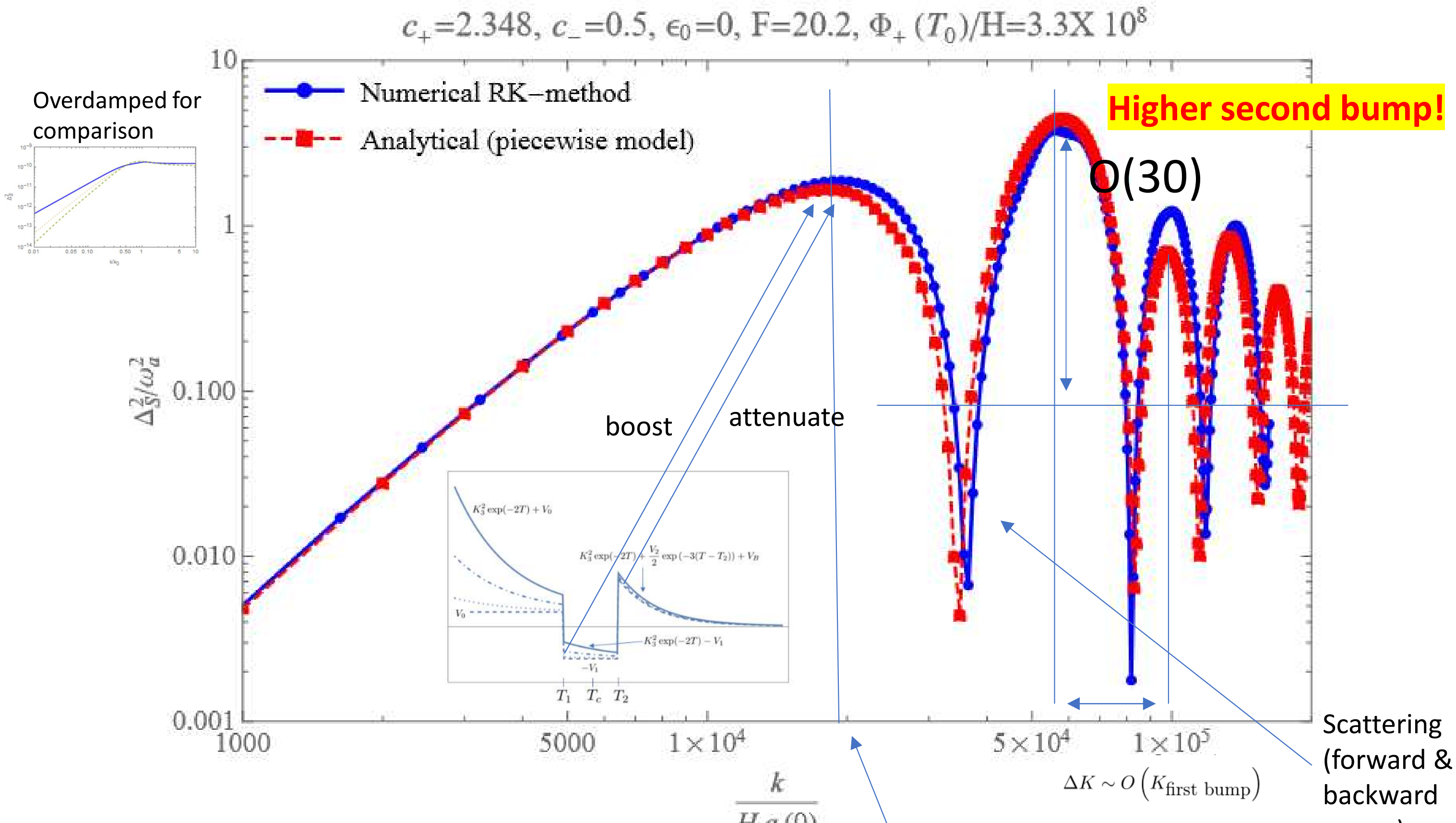

$$\alpha = \frac{\phi_+(0)}{F^2}\sqrt{\omega^2+(3/2+\epsilon_0)^2}e^{-3/2[\frac{1}{\omega}\left(\frac{\pi}{2}+\arctan\frac{3/2+\epsilon_0}{\omega}\right)]}$$

$$\frac{k}{a(0)H} \approx 2e^{T_2}$$

$$\frac{k_\star}{a_0} \sim \left(\frac{\varphi_{\text{init}}}{0.3M_p}\right)^{\frac{2}{3}} e^{-(N_e-50)}\left(\frac{T_{\text{rh}}/H}{10^{-1}}\right)^{1/3}\left(\frac{H/\varphi_{\text{fin}}}{10^{-3}}\right)^{2/3}(10\text{Mpc}^{-1})$$

Other interesting points of note:

- There is good prospects for seeing the break in future experiments since the break scale cannot be pused too far naturally.

$$\frac{k_\star}{a_0} \sim \left(\frac{\varphi_{\rm init}}{0.3M_p}\right)^{\frac{2}{3}} e^{-(N_e-50)} \left(\frac{T_{\rm rh}/H}{10^{-1}}\right)^{1/3} \left(\frac{H/\varphi_{\rm fin}}{10^{-3}}\right)^{2/3} (10\,{\rm Mpc}^{-1})$$

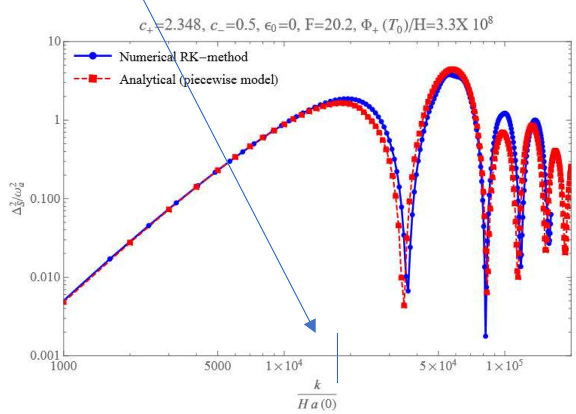

- One may be able to experimentally see these even if they make up a tiny (e.g. 10^{-4}) fraction of the dark matter.

Blue isocurvature may be discoverable in the future

How much sensitivity is there for discovery in future data?

w/ Tadepalli + Muenchmeyer

We will try to answer this in the context of couple of upcoming experiments [2306.09456]:

Euclid and MegaMapper (MM)

First approximation: ignore the "break" in the spectrum

Generically, there has to be a break in the spectrum: otherwise dark matter will dilute away. [1509.05850]

However, as a warmup, we consider only a power law isocurvature here [2306.09456].

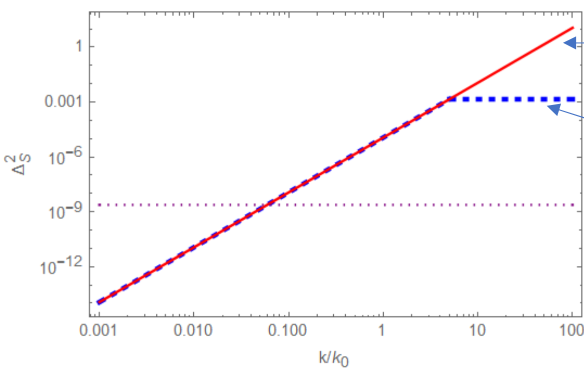

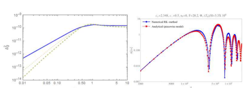

$$\frac{k^3}{2\pi^2} P_{S_{cdm}}(k) = A_{\rm iso}(k_{\rm p}) \left(\frac{k}{k_{\rm p}}\right)^{n_{\rm iso}-1}$$

$$\frac{k^3}{2\pi^2} P_{\mathcal{R}}(k) = A_{\rm ad}(k_{\rm p}) \left(\frac{k}{k_{\rm p}}\right)^{n_{\rm ad}-1}$$

Main parameter that will be constrained $\alpha = \dfrac{A_{\rm iso}(k_{\rm p})}{A_{\rm ad}(k_{\rm p})}$

Why Euclid and Megamapper?

Linear theoretical predictions are arguably easier to test and **higher redshifts** allow more linear data volume.

Details:

Dark matter clustering $\delta(k)$:

Larger k modes enter the horizon earlier and grow as $\delta(k) \propto a$

↓

Larger k modes become larger first reaching nonlinearity

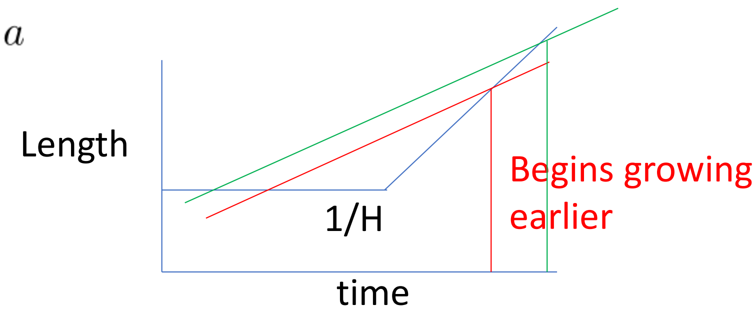

$$\delta(k) \sim \frac{k^2}{k_{\rm NL}^2(z)}$$

$$k_{\rm NL} \sim 0.3h\,{\rm Mpc}^{-1}\sqrt{1+z}$$

Naively, better theory control of high k clustering with higher redshifts z

Some next generation of experiments are probing higher redshifts.

[2106.09713]

Volume measure

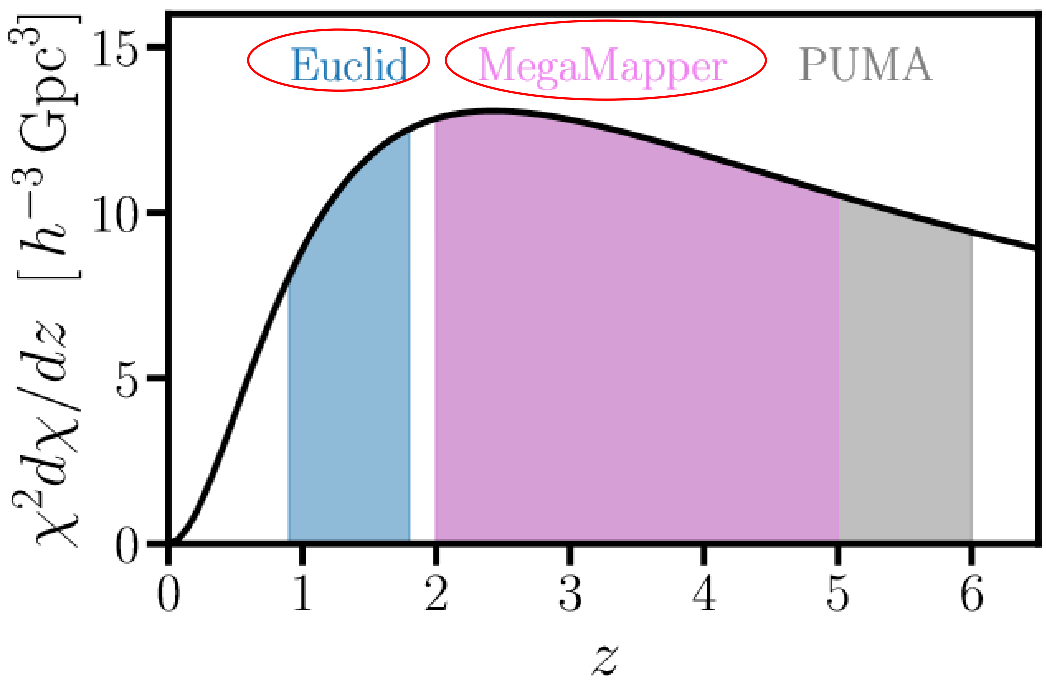

Comoving volume per redshift

$$\chi(a) = \int_{t(a)}^{t_0} \frac{dt'}{a(t')}$$

2106.09713

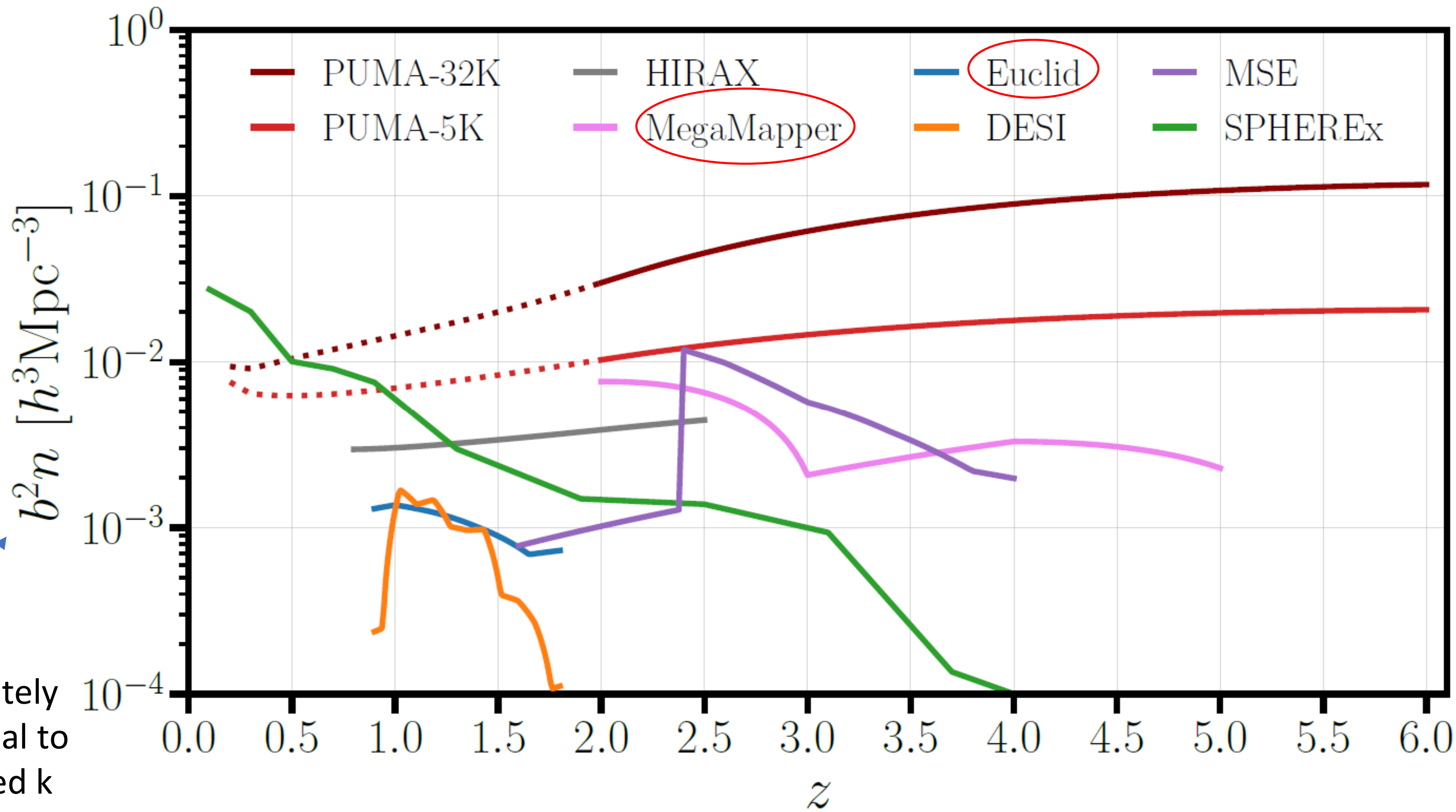

Approximately proportional to S/N for fixed k

Euclid [1110.3193]

Near-IR space telescope
Coverage: 15,000 square degrees
Angular resolution: 5 X 10^{-6} radians

$$\frac{k_{\max}}{a_0} \sim 50h\mathrm{Mpc}^{-1}$$

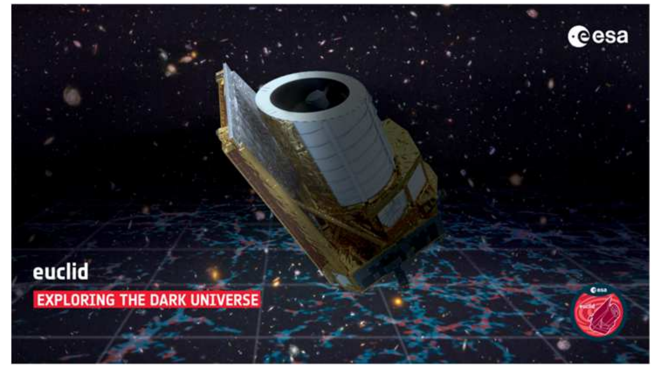

https://www.esa.int/Science_Exploration/Space_Science/Euclid_overview

Target: z range: 1-2
$\mathrm{H}\alpha$ emitter galaxies
(i.e. young star forming small galaxies, far away)

Instrument special features:

highly calibrated imaging system → weak lensing
good spectroscopy → baryon acoustic oscillations

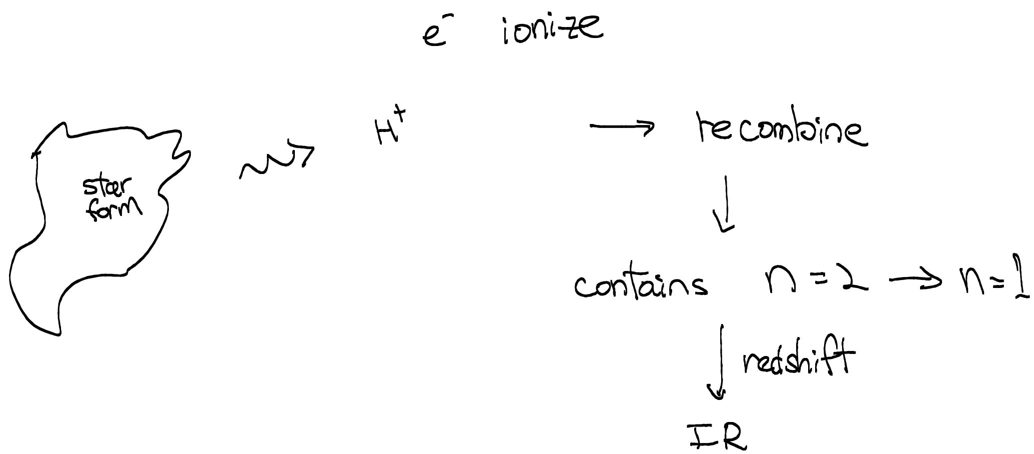

Euclid [1110.3193]

Near-IR space telescope
Coverage: 15,000 square degrees
Angular resolution: 5 X 10^{-6} radians

$$\frac{k_{\max}}{a_0} \sim 50 h \mathrm{Mpc}^{-1}$$

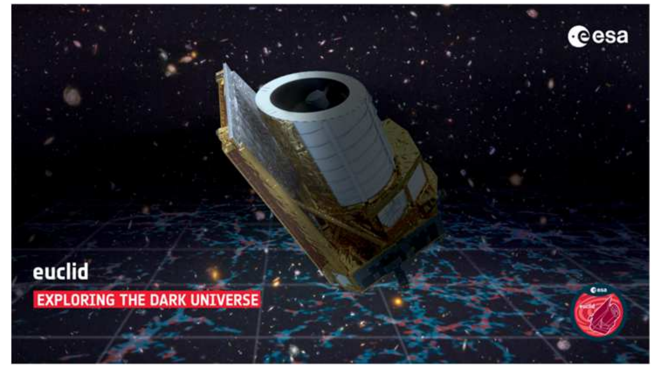

https://www.esa.int/Science_Exploration/Space_Science/Euclid_overview

Target: z range: 1-2
$H\alpha$ emitter galaxies
(i.e. young star forming small galaxies, far away)

Instrument special features:

highly calibrated imaging system → weak lensing
good spectroscopy → baryon acoustic oscillations

Cost: ~ $800 M (mostly ESA and around 50M from NASA)
https://spacenews.com/esa-panel-gives-final-approval-euclid-space-telescope/

The launch

Launch period: July 2023

Launch location: Cape Canaveral, Florida, USA

Launch vehicle: SpaceX Falcon 9

Destination: Sun-Earth Lagrange point 2, 1.5 million km from Earth

Megamapper concept [1907.11171, 2209.04322]

Ground-based Magellan-like telescope (Chile): 6.5m
2< z < 5

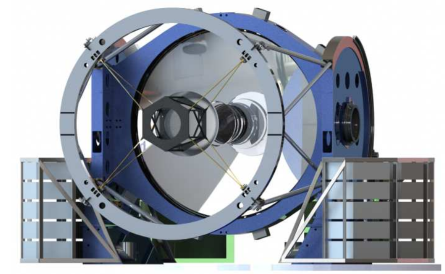

Target: z range 2-5
Lyman break galaxies

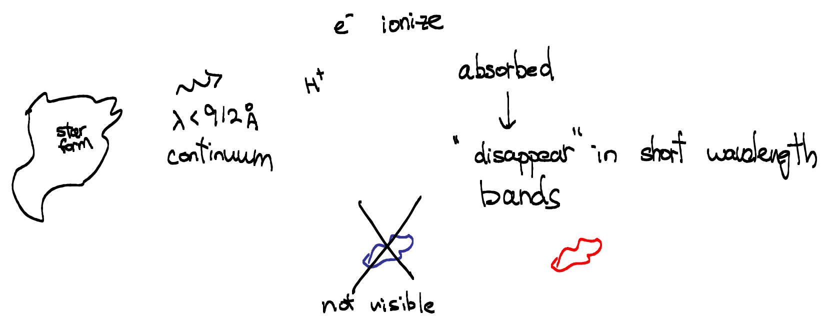

Instrument special features:

Wide field coupled with DESI spectrographs
Small-pitch robots to achieve multiplexing of 26,100

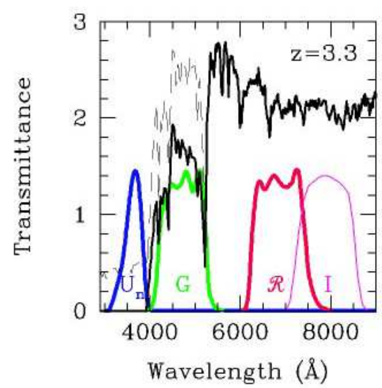

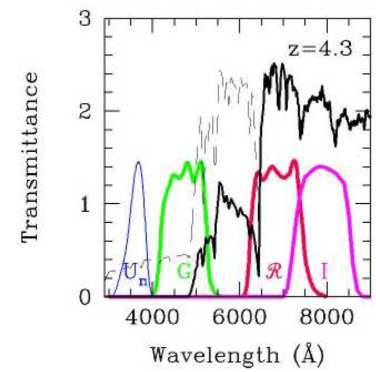

Megamapper concept [1907.11171, 2209.04322]

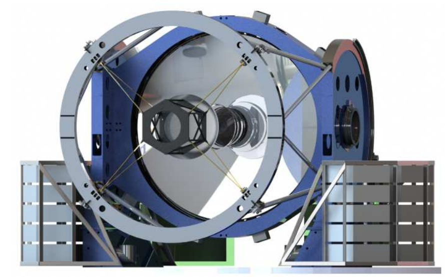

Ground-based Magellan-like telescope (Chile): 6.5m
2< z < 5

Target: z range 2-5
Lyman break galaxies

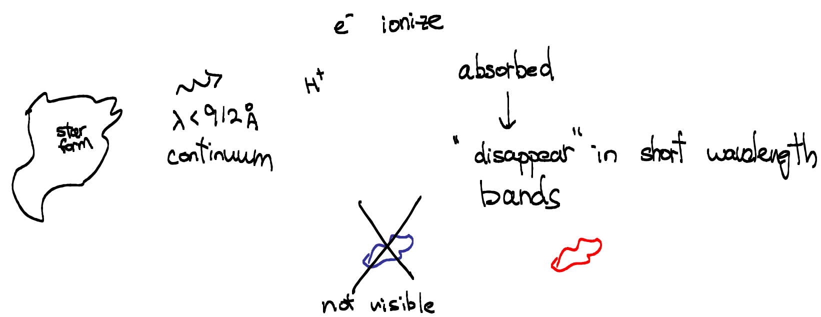

Instrument special features:

Wide field coupled with DESI spectrographs
Small-pitch robots to achieve multiplexing of 26,100

Estimated cost: $140 M

Back to our question:

What may be the constraint/signal on the isocurvature amplitude and spectral index provided by Euclid and MM which represent near future large scale structure observational reach?

Use Fisher forecast to answer this with theoretical prediction encoded with EFTofLSS:

$$F_{ij} = -\left\langle \frac{\partial^2 \ln \mathcal{L}}{\partial p_i \partial p_j} \right\rangle \Bigg|_{p=p_{\rm fid}}$$

$$F = F^p + F^b + \mathrm{diag}\left(\sigma_{p_i}^{-2}\right)$$

Galaxy power spectrum (F^p)

Bispectrum (F^b)

prior ($\mathrm{diag}\left(\sigma_{p_i}^{-2}\right)$)

$$F = F^p + F^b + \mathrm{diag}\left(\sigma_{p_i}^{-2}\right)$$

Example: power spec Fisher matrix

Expected galaxy power spectrum

$$F_{ij}^s = \sum_{z_l} \sum_{k,k'} \frac{\partial P_s(k, z_l)}{\partial p_i} \left(C^{-1}(z_l)\right)_{kk'}^s \frac{\partial P_s(k', z_l)}{\partial p_j}$$

parameters

$$C_{kk'}^s(z_l) = C_{d,kk'}^s(z_l) + C_{e,kk'}^s(z_l)$$

Error envelope

Experiment information:
e.g. Euclid vs MM

Theory error

$$C_{e,kk'}^s(z_l) = E_k^s \exp\left[-\frac{(k-k')^2}{2\Delta k^2}\right] E_{k'}^s$$

To make the forecast, one has to have a sufficiently small theory error at k values of interest for the experiments at hand.

We use EFTofLSS and bias expansion to compute the theory.

Computing the theoretical predictions in [2306.09456]:

[1004.2488, 1206.2926, 1909.05271] EFTofLSS: A systematically constructed fitting function that can splice together perturbation theory and numerical simulations

[1104.2933,2004.10607] CLASS-PT: Linear power spec at z=99

[1603.00476] FastPM: Nbody: particle positions and vel

[1712.05834] NbodyKit: matter power spectra
Halo model: FOF
Galaxy model: HOD

EFTofLSS

$$\delta = \delta^{(1)} + \delta^{(2)} + \delta^{(3)} - c^2\nabla^2\delta^{(1)} + \epsilon_{\rm m}$$

IR= SPT + use P_{11} from CLASS-PT for IR resummation

EFT c^2 calibrate

Compute power spectrum (accurate to 4th order in $\delta^{(1)}$ ←→ note derivative = $\delta^{(1)}$)

$$P_{\rm NL}(k,z) = P_{11}(k,z) + [P_{22}(k,z) + P_{13}(k,z)] - 2c^2(z)k^2 P_{\rm lin}(k,z) + P_{\Delta\tau}(k,z)$$

e.g. $P_{13} \leftrightarrow \left\langle \delta^{(1)}\delta^{(3)} \right\rangle$

Feed this into bias expansion [review 1611.09787]

Galaxy: $\delta_g(x) = \sum_O (b_O + \epsilon_O(x))\, O(x) + b_\epsilon \epsilon(x)$

Adjust c^2 to match Nbody

EFTofLSS

[1004.2488, 1206.2926]

Main advantages of using EFTofLSS:

1) Systematics are well understood
2) Easy to adapt to isocurvature

Idea: A) coarse grain the equation of motion → separates UV terms and IR terms
B) parameterize UV effective terms that can be matched to N-body simulations

Fluctuations of fields are statistical ←→ this is the QFT-like part

However, **all statistical propagator-analogs of QFT are spacelike in the EFTofLSS: i.e. "propagators" are not Green's functions**

The time evolution is **deterministic** [i.e. in contrast with QFT] ←→ Hence, time evolution is a **constraint** rather than fluctuation dynamics from a QFT analogy perspective

Math: $\delta_l(\vec{x})$ similar to composite operator definition in statistical field theory in the context of a Wilsonian EFT

$$\delta_l = \delta_l[\delta(t_i, \vec{x})]$$

This is not analogous to

$$\varphi = \overline{T}\left[e^{i\int_{-\infty}^{t} dt' H_I[\varphi_I]}\right]\varphi_I(t,\vec{x})T\left[e^{-i\int_{-\infty}^{t} dt' H_I[\varphi_I]}\right]$$

since the time evolution is independent of the statistical correlators in the EFTofLSS unlike here

Symmetries of the system: Galilean group + Lifshitz scaling type
[1301.7182,1505.06668]

Effective Euler:

$$\rho_l(\vec{x})\left(\partial_\tau v_l(\vec{x}) + \mathcal{H} v_l(\vec{x}) + v_l^j(\vec{x})\partial_j v_l(\vec{x}) + \partial_i \phi_l(\vec{x})\right) \approx -\partial_j \left[\tau_i^j\right]_\Lambda$$

$$\left[\tau_i^j\right]_\Lambda = \left[\rho(\vec{x}')v_{si}(\vec{x}')v_s^j(\vec{x}') + \frac{2\partial^j\phi_s(\vec{x}')\partial_i\phi_s(\vec{x}') - \delta_i^j\partial^f\phi_s(\vec{x}')\partial_f\phi_s(\vec{x}')}{8\pi G}\right]_\Lambda$$

parameterize terms that will enter correlation computations using a combination of perturbativity and derivative power counting

Isotropic pressure sound speed

$$c_s^2 \equiv \frac{\left\langle \frac{1}{3}\left[\tau^k_k\right]_\Lambda \delta_l \right\rangle}{\rho_0 \left\langle \delta_l \delta_l \right\rangle}$$

"viscosity" coefficient

$$c_{\text{vis}}^2 \equiv \frac{\left\langle \delta_l \left(\frac{\partial_i\partial_j}{\rho_0\nabla^2}\left[\tau^{ij}\right]_\Lambda\right)\right\rangle}{\left\langle \delta_l \delta_l \right\rangle}$$

$$\left(c_s^{\text{SI}}\right)^2 \approx c_s^2 \times O(1) \times 10^{-5} c_{\text{light}}^2$$

Effective parameter that enters computations

$$c^2 \approx c_s^2 + c_{\text{vis}}^2$$

Effective composite operator:

$$\delta = \delta^{(1)} + \delta^{(2)}[\delta^{(1)}] + \delta^{(3)}[\delta^{(1)}] - c^2\left(z, \left\langle \delta^{(1)}\delta^{(1)} \right\rangle_{z_{\text{early}}}\right)\nabla^2\delta^{(1)} + \epsilon_m$$

[drop "l" subscript]

Initial power spectrum dependence

Divergence structure is different than in the adiabatic case

Field theory intuition: perturbative propagator ←→ linear power spectrum P_{11}

Mixed = adiabatic + Blue isocurvature →

$$P_{\rm lin}^{\rm MX}(k, z \ll z_{\rm eq}) = P_{\rm lin}^{\rm AD}(k, z) + P_{\rm lin}^{\rm ISO}(k, z)$$
$$\approx P_{\rm lin}^{\rm AD}(k, z) \left(1 + \alpha \left(\frac{f_c}{3}\right)^2 \left(\frac{T_{\rm iso}(k)}{T_{\rm ad}(k)}\right)^2 \left(\frac{k}{k_{\rm p}}\right)^{n_{\rm iso} - n_{\rm ad}}\right)$$

$$\alpha = \frac{A_{\rm iso}(k_{\rm p})}{A_{\rm ad}(k_{\rm p})}$$

1-loop

$$P_{13}^{\rm UV}(k) \approx -k^2 P_{11}(k) \frac{61}{630\pi^2} \int^{\Lambda} dq P_{11}(q)$$
$$\sim -10^{-2} k^2 P_{11}(k) \Lambda^{n_{\rm iso} - 3}$$

One major departure from adiabatic:

Divergent for $n_{\rm iso} \geq 3$

[convergent for $n_{\rm iso} \to n_{\rm ad} = 1$]

Divergence structure is different than in the adiabatic case

Field theory intuition: perturbative propagator ←→ linear power spectrum P_{11}

Mixed = adiabatic + Blue isocurvature →

$$P_{\rm lin}^{\rm MX}(k, z \ll z_{\rm eq}) = P_{\rm lin}^{\rm AD}(k,z) + P_{\rm lin}^{\rm ISO}(k,z)$$
$$\approx P_{\rm lin}^{\rm AD}(k,z)\left(1+\alpha\left(\frac{f_c}{3}\right)^2\left(\frac{T_{\rm iso}(k)}{T_{\rm ad}(k)}\right)^2\left(\frac{k}{k_{\rm p}}\right)^{n_{\rm iso}-n_{\rm ad}}\right)$$

$$\alpha = \frac{A_{\rm iso}(k_{\rm p})}{A_{\rm ad}(k_{\rm p})}$$

1-loop

$$P_{13}^{\rm UV}(k) \approx -k^2 P_{11}(k)\frac{61}{630\pi^2}\int^{\Lambda} dq P_{11}(q)$$
$$\sim -10^{-2} k^2 P_{11}(k)\Lambda^{n_{\rm iso}-3}$$

One major departure from adiabatic:

Divergent for $n_{\rm iso} \geq 3$

[convergent for $n_{\rm iso} \to n_{\rm ad} = 1$]

→ Counter term separation at 1-loop

$$\delta = \delta^{(1)} + \delta^{(2)} + \delta^{(3)} - c^2\nabla^2\delta^{(1)} + \epsilon_{\rm m}$$
$$c^2(z) = c^2_{\rm ren}(k_{\rm ren}, z) + c^2_{\Lambda}(z)$$

Renormalization scheme determining $c^2_\Lambda(z)$: $c^2(z) = c^2_{\mathrm{ren}}(k_{\mathrm{ren}}, z) + c^2_\Lambda(z)$

$$\left\langle [O_i](\vec{k})\delta^{(1)}(\vec{k}_1)\cdots\delta^{(1)}(\vec{k}_n)\right\rangle = \left\langle O_i(\vec{k})\delta^{(1)}(\vec{k}_1)\cdots\delta^{(1)}(\vec{k}_n)\right\rangle_{\mathrm{tree}} \qquad \forall k_i \longrightarrow 0$$

[Not at zero but tending to zero]

Independent of Λ

Fixing the finite value $c^2_{\mathrm{ren}}(k_{\mathrm{ren}}, z)$: Match to N-body at $k_{\mathrm{ren}} = 0.1\mathrm{h/Mpc}$

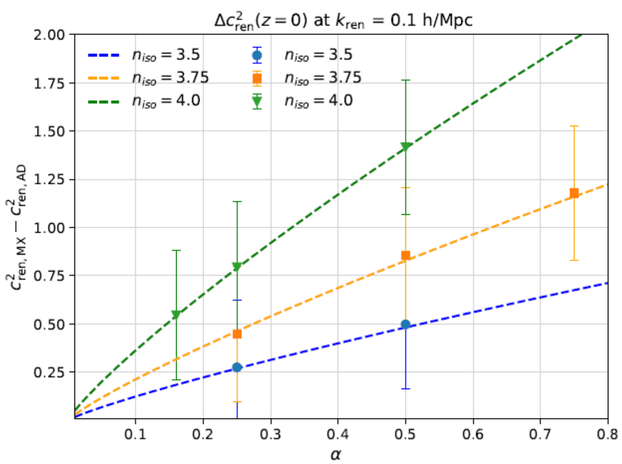

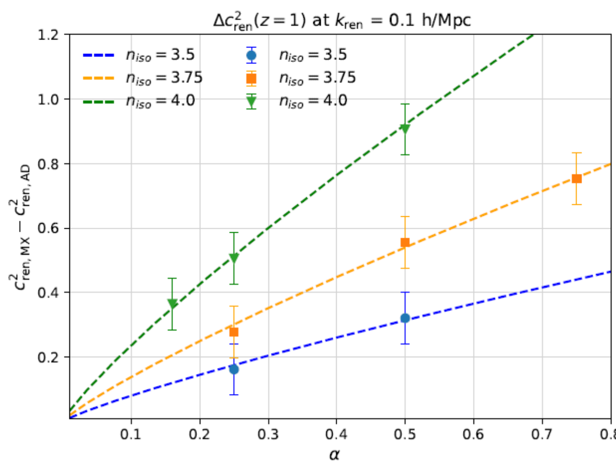

$$\alpha = \frac{A_{\mathrm{iso}}(k_{\mathrm{p}})}{A_{\mathrm{ad}}(k_{\mathrm{p}})}$$

Mixed adiabatic + isocurvature

$$\delta = \delta^{(1)} + \delta^{(2)}[\delta^{(1)}] + \delta^{(3)}[\delta^{(1)}] - c^2\left(z, \left\langle \delta^{(1)}\delta^{(1)}\right\rangle_{z_{\mathrm{early}}}\right)\nabla^2\delta^{(1)} + \epsilon_m$$

Renormalization scheme determining $c^2_\Lambda(z)$: $c^2(z) = c^2_{\rm ren}(k_{\rm ren}, z) + c^2_\Lambda(z)$

$$\left\langle [O_i](\vec{k})\delta^{(1)}(\vec{k}_1)\cdots\delta^{(1)}(\vec{k}_n)\right\rangle = \left\langle O_i(\vec{k})\delta^{(1)}(\vec{k}_1)\cdots\delta^{(1)}(\vec{k}_n)\right\rangle_{\rm tree} \qquad \forall k_i \to 0$$

[Not at zero but tending to zero]

Independent of Λ

Fixing the finite value $c^2_{\rm ren}(k_{\rm ren}, z)$: Match to N-body at $k_{\rm ren} = 0.1 {\rm h/Mpc}$

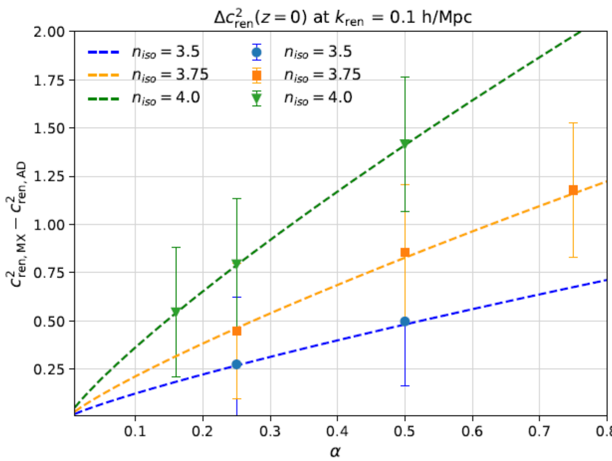

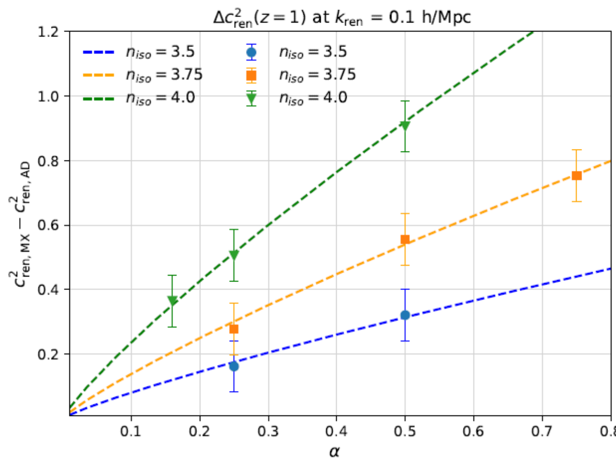

$$\alpha = \frac{A_{\rm iso}(k_{\rm p})}{A_{\rm ad}(k_{\rm p})}$$

Mixed adiabatic + isocurvature

$$\delta = \delta^{(1)} + \delta^{(2)}[\delta^{(1)}] + \delta^{(3)}[\delta^{(1)}] - c^2\left(z, \left\langle \delta^{(1)}\delta^{(1)}\right\rangle_{z_{\rm early}}\right)\nabla^2\delta^{(1)} + \epsilon_m$$

Recall c^2 is one of the key feature of EFTofLSS

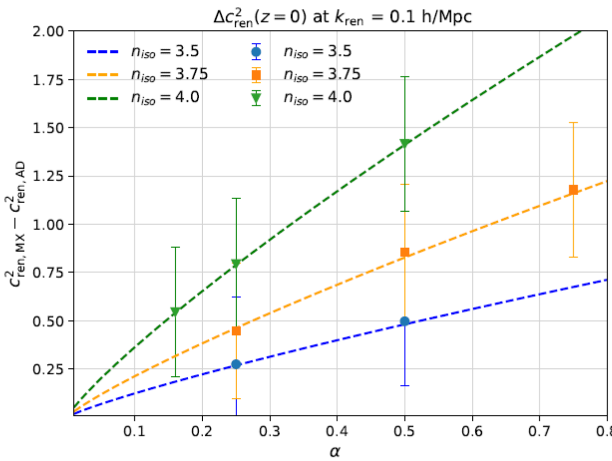

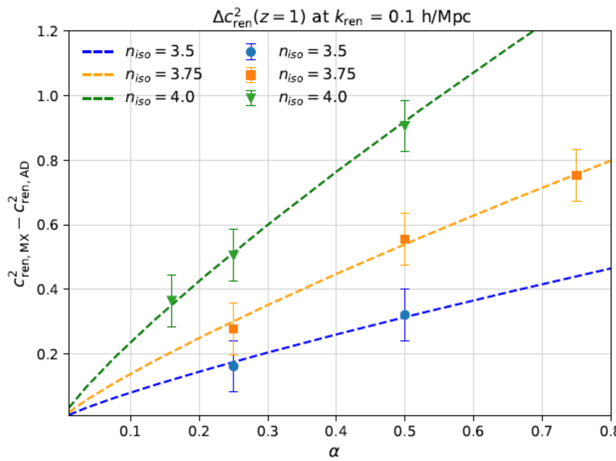

[2306.09456]

$$c^2_{\rm ren,MX}(k_{\rm ren},z) - c^2_{\rm ren,AD}(k_{\rm ren},z) \approx \frac{P^{\rm AD}_{\rm 1-EFT}(k_{\rm ren},z)}{P^{\rm AD}_{11}(k_{\rm ren},z)} \times \frac{\alpha\left(\frac{f_c}{3}\right)^2\left(\frac{T_{\rm iso}(k_{\rm ren})}{T_{\rm ad}(k_{\rm ren})}\right)^2\left(\frac{k_{\rm ren}}{k_{\rm p}}\right)^{n_{\rm iso}-n_{\rm ad}}}{1+\alpha\left(\frac{f_c}{3}\right)^2\left(\frac{T_{\rm iso}(k_{\rm ren})}{T_{\rm ad}(k_{\rm ren})}\right)^2\left(\frac{k_{\rm ren}}{k_{\rm p}}\right)^{n_{\rm iso}-n_{\rm ad}}} \times$$
$$\left(0.284\, D(z)^{0.858}\alpha^{-0.147}\,(n_{\rm iso}-n_{\rm ad})\left(\frac{k_s}{k_{\rm p}}\right)^{n_{\rm iso}-n_{\rm ad}}\right)$$

$$k_s \approx k_* \approx 0.2174\ {\rm Mpc}^{-1}$$

$$k_{\rm p} = 0.05\,{\rm Mpc}^{-1}$$

EFTofLSS is a good fitting formalism to N-Body for mixed initial conditions as well

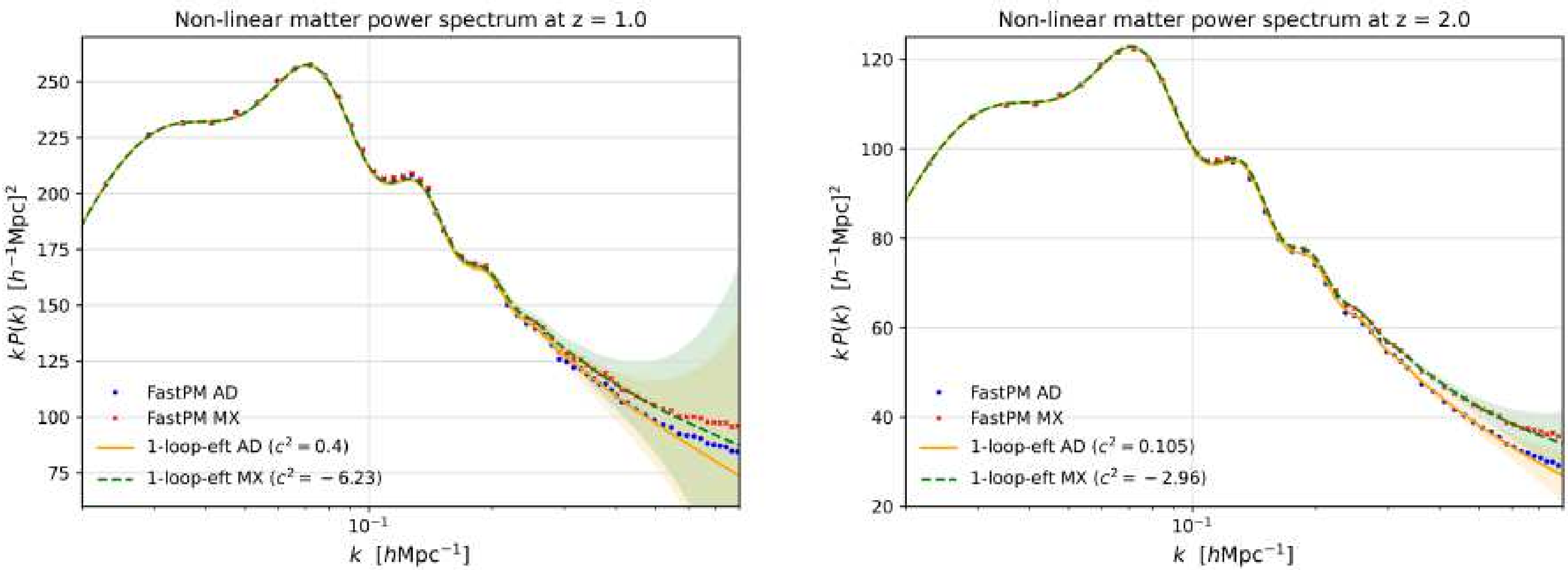

[2306.09456]

Bias expansion

[1402.5916, 1611.09787]

Galaxy is a composite operator of the density field:

$$\delta_g(x) = b_1\delta(x) + b_\epsilon\epsilon(x) + \frac{b_2}{2}\delta^2(x) + b_{\mathcal{G}_2}\mathcal{G}_2(x) + \epsilon_\delta(x)\delta(x) + b_{\delta\mathcal{G}_2}\delta(x)\mathcal{G}_2(x)$$
$$+ \frac{b_3}{6}\delta^3(x) + b_{\mathcal{G}_3}\mathcal{G}_3(x) + b_{\Gamma_3}\Gamma_3(x) + \epsilon_{\delta^2}(x)\delta^2(x) + \epsilon_{\mathcal{G}_2}(x)\mathcal{G}_2(x)$$
$$+ b_{\nabla^2\delta}\nabla^2\delta(x) + b_{\nabla^2\epsilon}\nabla^2\epsilon(x)$$

2-point function of this operator at 1-loop:

$$\left\langle \frac{\delta n_{\rm galaxy}}{n_{\rm galaxy}} \frac{\delta n_{\rm galaxy}}{n_{\rm galaxy}} \right\rangle \longrightarrow P_{gg}(k) = b_1^2 P_{\rm NL}(k) + P_{gg}^{\rm NLO}(k) + P_{gg,\nabla^2\delta}(k) + P_{gg,\epsilon}(k)$$

$$P_{\rm NL} = P_{11} + P_{22} + P_{13} - 2c^2k^2P_{11}$$

$$P_{gg}^{\rm NLO} = b_1\left(b_2\mathcal{I}_{\delta^{(2)}\delta^2}(k) + 2b_{\mathcal{G}_2}\mathcal{I}_{\delta^{(2)}\mathcal{G}_2}(k) + \left(2b_{\mathcal{G}_2} + \frac{4}{5}b_{\Gamma_3}\right)\mathcal{F}_{\mathcal{G}_2}\right)$$
$$+ b_2 b_{\mathcal{G}_2}\mathcal{I}_{\delta^2\mathcal{G}_2}(k) + \frac{1}{4}b_2^2\mathcal{I}_{\delta^2\delta^2}(k) + b_{\mathcal{G}_2}^2\mathcal{I}_{\mathcal{G}_2\mathcal{G}_2}(k)$$

$$P_{gg,\nabla^2\delta}(k) = -2b_1 b_{\nabla^2\delta}\left(\frac{k}{k_*}\right)^2 P_{11}(k)$$

$$P_{gg,\epsilon}(k) = P_{\epsilon\epsilon}b_\epsilon\left(1 + 2b_{\nabla^2\epsilon}\left(\frac{k}{k_*}\right)^2\right)$$

Novel cutoff sensitivity of bias counter-terms arise just as for the EFTofLSS sound speed

This Laplacian bias will be significant in terms of generating degeneracies because of k dependence.

3-point function at tree level:

$$\left\langle \frac{\delta n_{\rm galaxy}}{n_{\rm galaxy}} \frac{\delta n_{\rm galaxy}}{n_{\rm galaxy}} \frac{\delta n_{\rm galaxy}}{n_{\rm galaxy}} \right\rangle \longrightarrow$$

$$B_{gg}\left(\vec{k}_1, \vec{k}_2, \vec{k}_3\right) = \left(F_2^b\left(\vec{k}_1, \vec{k}_2\right) b_1^2 P_{11}(k_1) P_{11}(k_2) + \text{cyclic}\right) + P_{\rm shot} \sum_{i=1}^{3} b_1^2 P_{11}(k_i) + B_{\rm shot}$$

$$F_2^b\left(\vec{k}_1, \vec{k}_2\right) = \frac{b_2}{2} + b_{\mathcal{G}_2}\left(\mu_{12}^2 - 1\right) + b_1\left(\frac{5}{7} + \frac{1}{2}\mu_{12}\left(\frac{k_1}{k_2} + \frac{k_2}{k_1}\right) + \frac{2}{7}\mu_{12}^2\right)$$

$$B_{\rm shot} = 1/\bar{n}_g^2$$

$$P_{\rm shot} = 1/\bar{n}_g$$

With respect to $\left\langle \frac{\delta n_{\rm galaxy}}{n_{\rm galaxy}} \frac{\delta n_{\rm galaxy}}{n_{\rm galaxy}} \right\rangle$ and $\left\langle \frac{\delta n_{\rm galaxy}}{n_{\rm galaxy}} \frac{\delta n_{\rm galaxy}}{n_{\rm galaxy}} \frac{\delta n_{\rm galaxy}}{n_{\rm galaxy}} \right\rangle$:

Because bias parameters are marginalized over, these are the primary limitations of the experimental sensitivity.

Back to the example: power spec Fisher matrix

Expected galaxy power spectrum

$$F_{ij}^{s} = \sum_{z_l} \sum_{k,k'} \frac{\partial P_s(k,z_l)}{\partial p_i} \left(C^{-1}(z_l)\right)^{s}_{kk'} \frac{\partial P_s(k',z_l)}{\partial p_j}$$

parameters

$$C^{s}_{kk'}(z_l) = C^{s}_{d,kk'}(z_l) + C^{s}_{e,kk'}(z_l)$$

Experiment information:
e.g. Euclid vs MM

Theory error

Error envelope

$$C^{s}_{e,kk'}(z_l) = E^{s}_{k} \exp\left[-\frac{(k-k')^2}{2\Delta k^2}\right] E^{s}_{k'}$$

[1602.00674]

error envelope estimating 2-loop part that was dropped:

$$E^{\mathrm{p}}_{\mathrm{gg}}(k,z) = (D_+(z)/D_+(0))^4\, P_{\mathrm{gg}}(k,z) \left(\frac{k}{0.45\,\mathrm{hMpc}^{-1}}\right)^{3.3}$$

The growth factor significantly changes the error

Error starts to become large near $k_{\mathrm{NL}} \approx 0.3\mathrm{h/Mpc}$

$$C^s_{d,kk'}(z_l) = \frac{(2\pi)^3}{V(z_l)} \frac{f_{\rm sky}^{-1}}{2\pi k^2 k_{\rm bin}} \left(P_s(k,z_l) + P_{s,\rm shot}(z_l)\right)^2 \delta_{kk'}$$

$$P_{\rm shot} = \frac{1}{\bar{n}_g}$$

1907.06666

Euclid parameters

$\bar{z}$	$V(\bar{z})$	$n_g(\bar{z})$	$V_{\rm eff}(\bar{z})$
0.6	4.58	3.83	4
0.8	6.44	2.08	4.98
1.0	8.01	1.18	5.09
1.2	9.23	0.7	4.37
1.4	10.15	0.39	2.98
1.6	10.81	0.21	1.55
1.8	11.25	0.12	0.68
2.0	11.53	0.07	0.28

$f_{\rm sky} \approx 0.35$

1903.09208

Fiducial parameter set for MM: realistically conservative

z	$n(z)$ [$10^{-4}\,h^3\,{\rm Mpc}^{-3}$]	$b(z)$		z	$n(z)$ [$10^{-4}\,h^3\,{\rm Mpc}^{-3}$]	$b(z)$
2.0	9.8	2.5		4.0	1.0	3.5
3.0	1.2	4.0		5.0	0.4	5.5

idealized parameter set for MM: magnitude-limited dropout sample with m_{UV} = 24.5

z	$n(z)$ [$10^{-4}\,h^3\,{\rm Mpc}^{-3}$]	$b(z)$		z	$n(z)$ [$10^{-4}\,h^3\,{\rm Mpc}^{-3}$]	$b(z)$
2.0	25	2.5		4.0	1.5	5.8
2.5	12	3.3		4.5	0.8	6.6
3.0	6.0	4.1		5.0	0.4	7.4
3.5	3.0	4.9				

Higher redshift is **not** always obviously better.

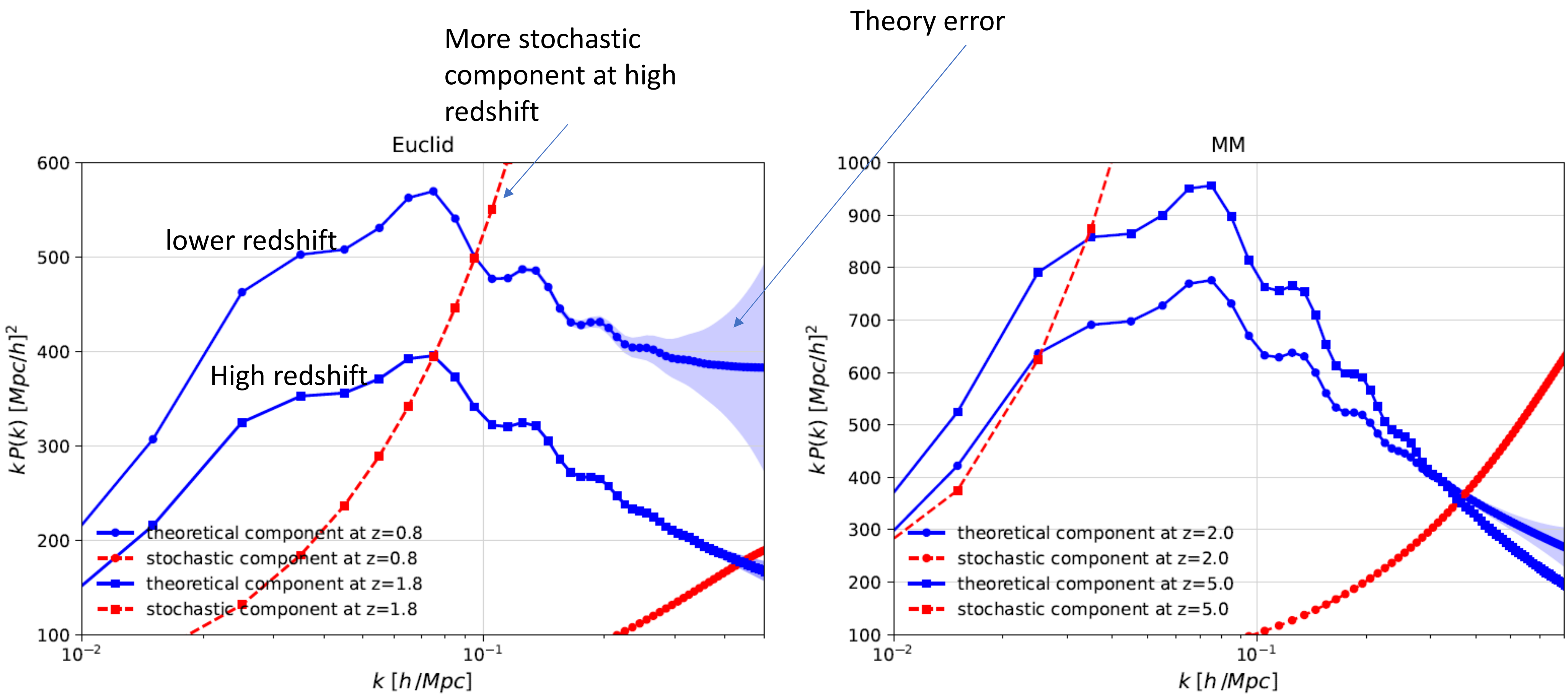

Higher redshift is not always obviously better.

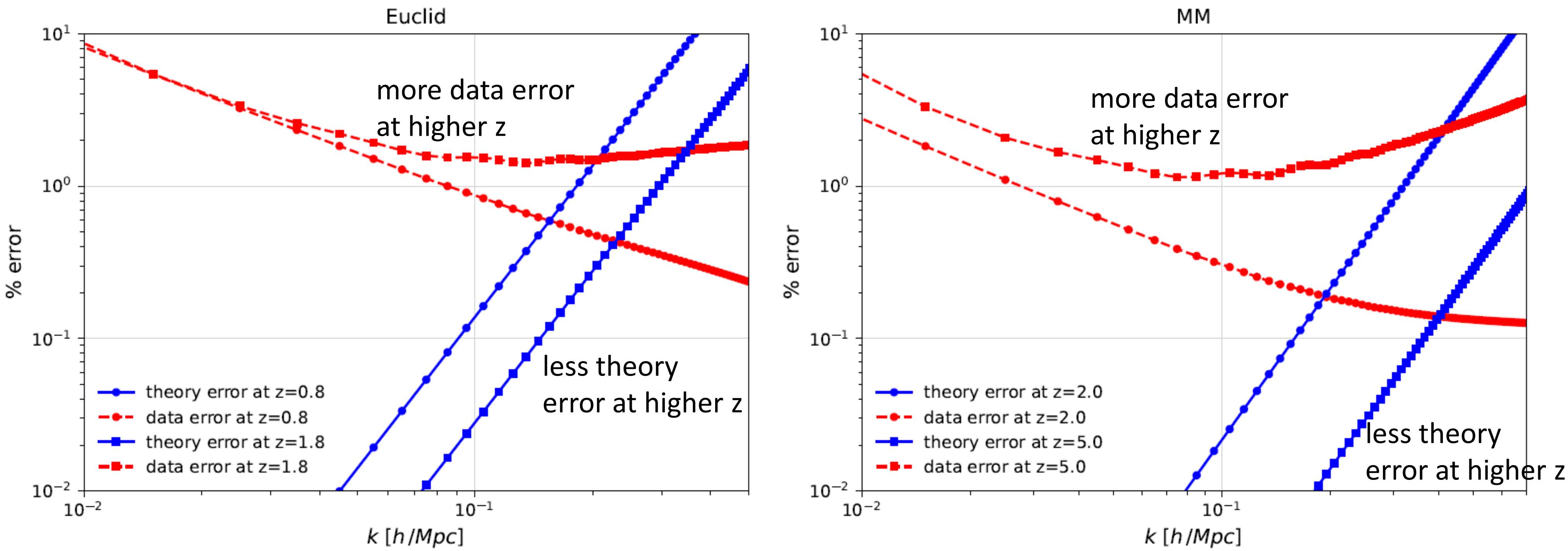

Better theory error will improve the sensitivity, but **bias** stands in the way.

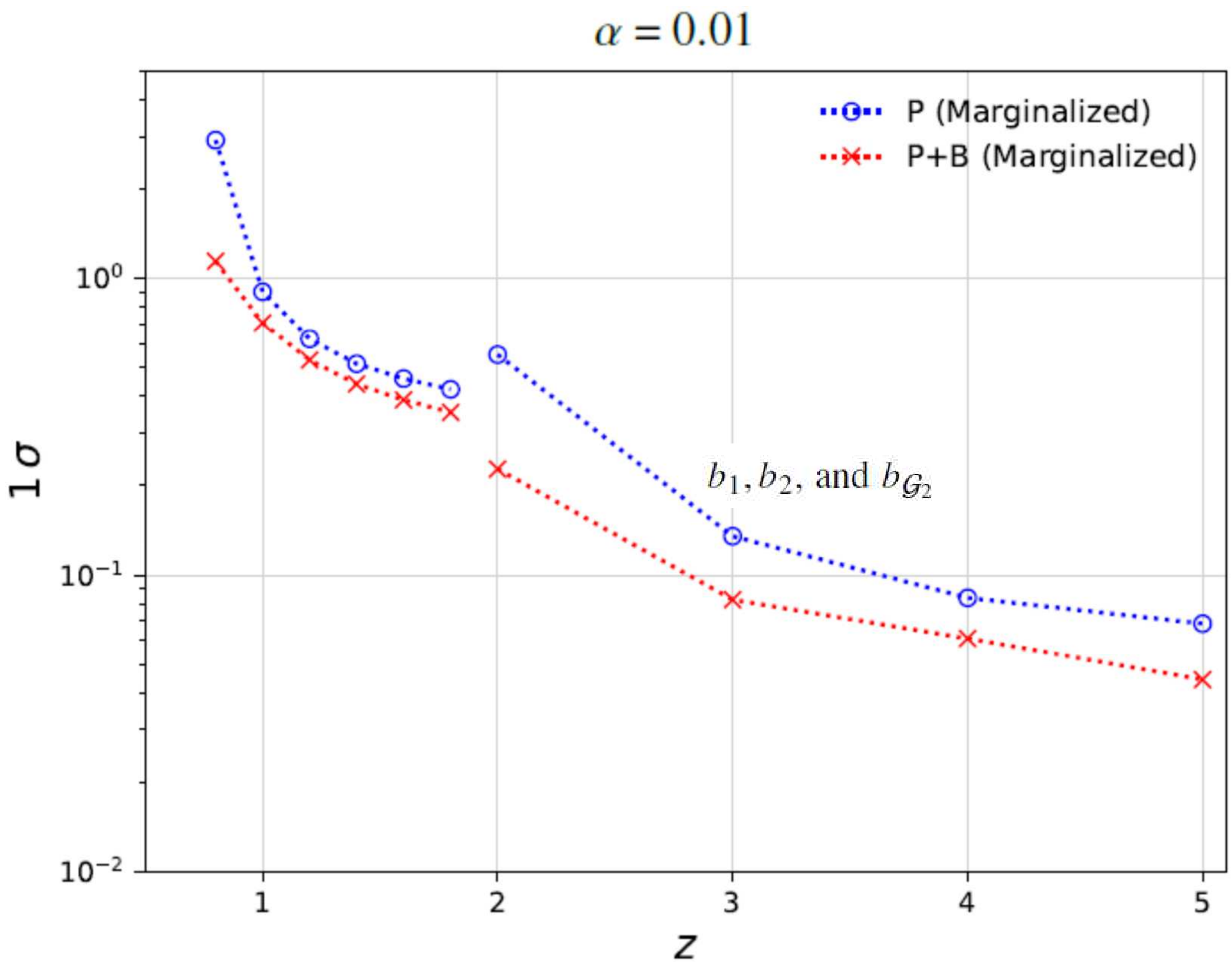

Improvement from the bispectrum is about as expected by breaking the degeneracy of

b_1, b_2, and $b_{\mathcal{G}_2}$

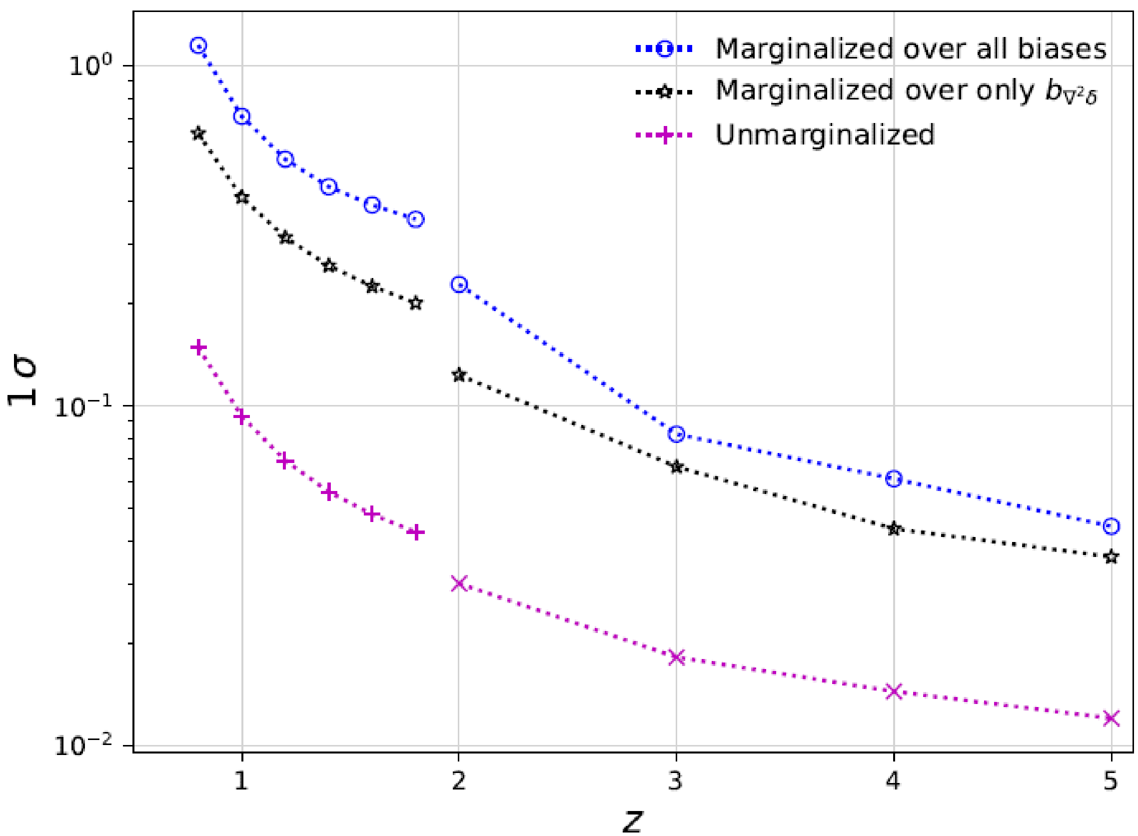

1) Most of the degradation in sensitivity comes from the Laplacian $b_{\nabla^2\delta}$

$$P_{gg,\nabla^2\delta}(k) = -2b_1 b_{\nabla^2\delta}\left(\frac{k}{k_*}\right)^2 P_{11}(k)$$

$$b_1 = \sqrt{1+z}$$

$$k_* \approx k_{\rm HD} \approx 0.4\,(D_+(z)/D_+(0))^{-4/3}\,({\rm h/Mpc})$$

A leading isocurvature term:

$$P_{gg} \supset b_1^2 P_{11}^{\rm AD}(k)\alpha\left(\frac{f_c}{3}\right)^2\left(\frac{T_{\rm iso}(k)}{T_{\rm ad}(k)}\right)^2\left(\frac{k}{k_{\rm p}}\right)^{n_{\rm iso}-n_{\rm ad}}$$

$$\propto b_1^2 \alpha P_{11}^{\rm AD}(k)\left(\frac{k}{k_{\rm p}}\right)^{n_{\rm iso}-n_{\rm ad}-0.5}$$

2) z dependence of bias term makes bias less degenerate for MM

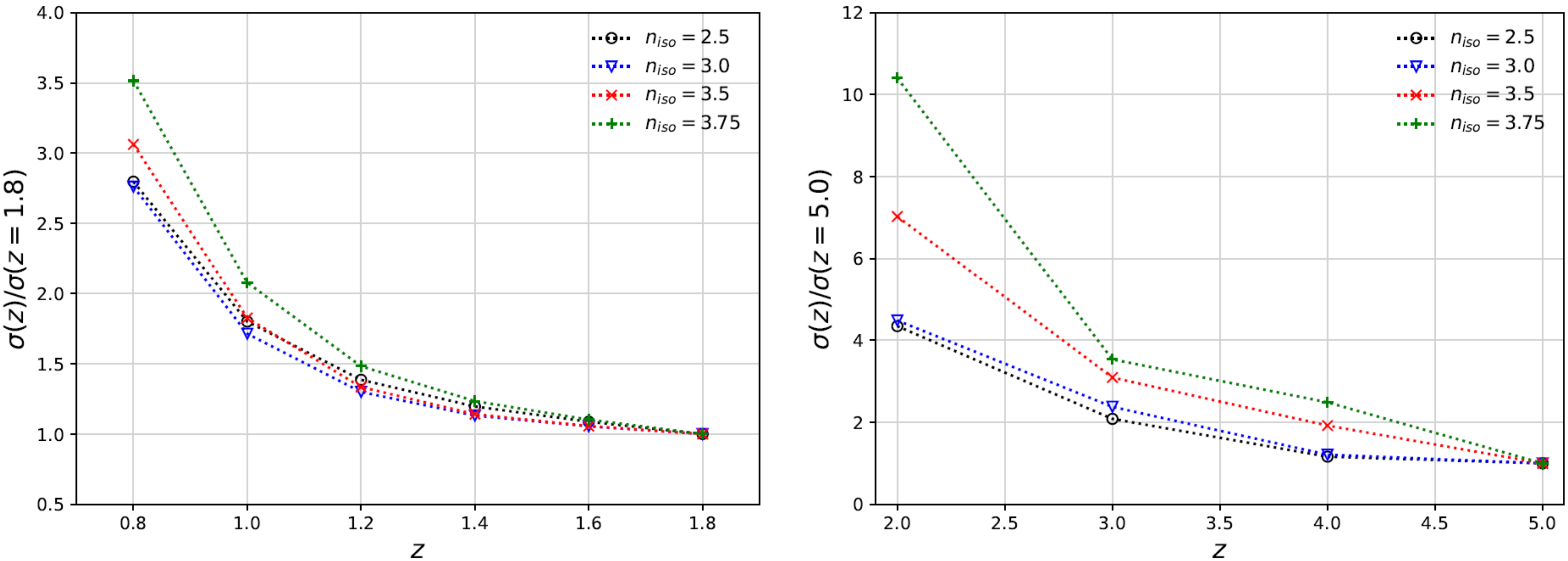

Larger k-range afforded by MM increases the sensitivity to different spectral indices.

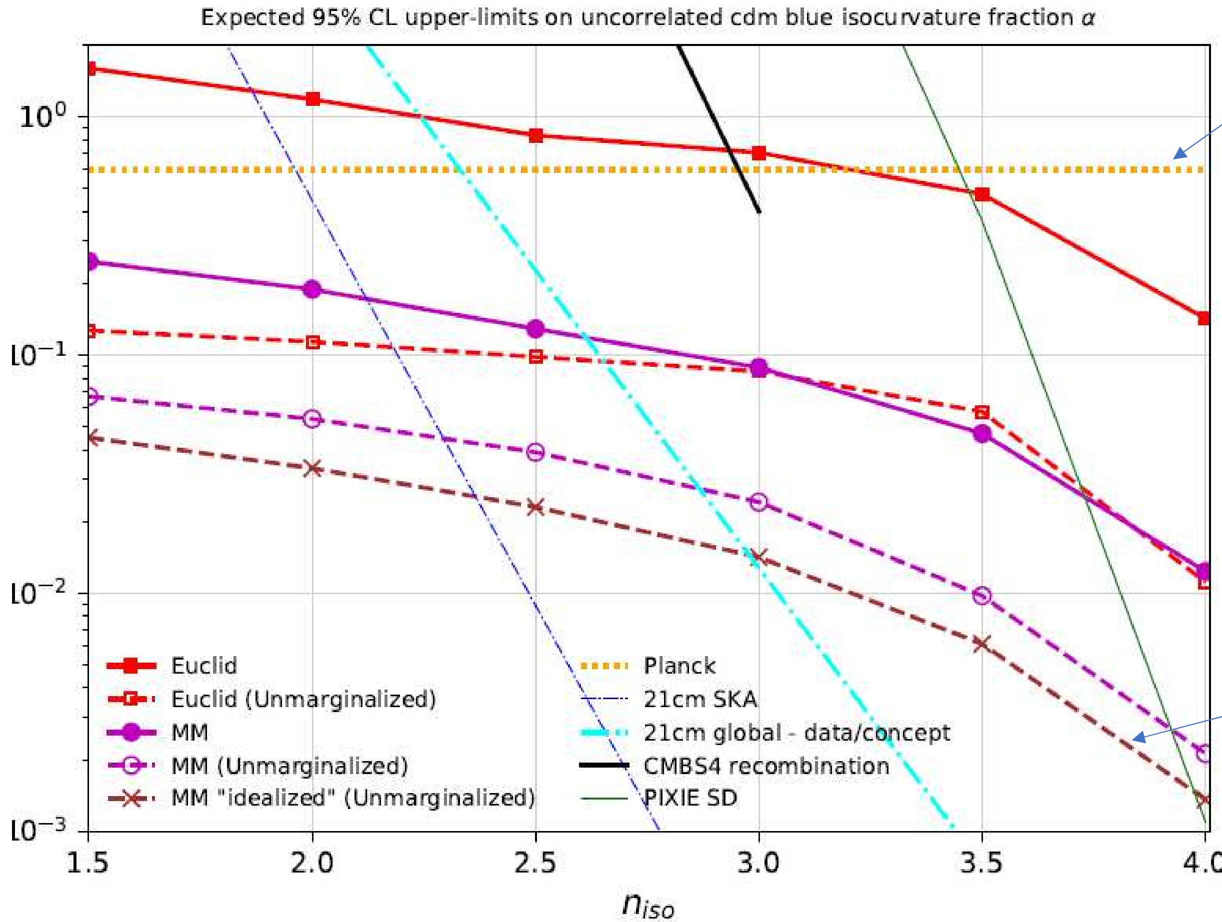

Existing bound

Idealized MM
m_{UV} = 24.5 magnitude
limited dropout sample

- Euclid can give a factor of few improvement for the high spectral index case
- MM can improve the $\alpha = \frac{A_{\rm iso}(k_{\rm p})}{A_{\rm ad}(k_{\rm p})}$ constraint by 1 to 1.5 orders of magnitude.

Future

- What is the prediction with a break in the spectrum (i.e. more realistic blue isocurvature)?
  - degeneracies will be broken → more sensitive
  - Less constraint from non-perturbative UV constraints (such as satellite galaxies)
- Put in redshift space distortion (will improve the degeneracy with bias parameters)
- Consider degeneracy of α with neutrino masses
- Non-perturbative constraints relying on semianalytic characterization of numerical simulations
- Computing bias parameters instead of marginalizing over them.

Summary

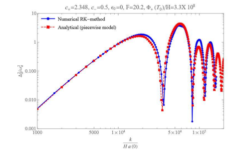

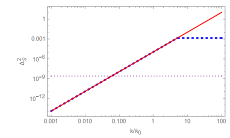

- Out of equilibrium axionic sector allows the generation of a rich UV primordial spectrum.
- A Fisher forecast was carried out for the Euclid and MM's sensitivity to blue powerlaw approximation of the isocurvature scenario.
- EFTofLSS at 1-loop $c^2_{\text{ren}}(k_{\text{ren}}, z)$ was fit to numerical results (CLASS-PT, FastPM, NbodyKit) to compute $\left\langle \frac{\delta n_{\text{galaxy}}}{n_{\text{galaxy}}} \frac{\delta n_{\text{galaxy}}}{n_{\text{galaxy}}} \right\rangle$ at 1-loop + $\left\langle \frac{\delta n_{\text{galaxy}}}{n_{\text{galaxy}}} \frac{\delta n_{\text{galaxy}}}{n_{\text{galaxy}}} \frac{\delta n_{\text{galaxy}}}{n_{\text{galaxy}}} \right\rangle$ at tree-level

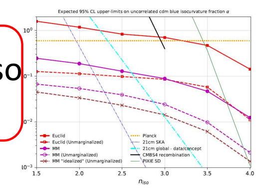

- Euclid → a factor of few improvements for the isocurvature amplitude at large n_{iso}
- MM → 1 to 1.5 order of magnitude improvement over current constraints
- The dominant degeneracy that limits the sensitivity of the experiments is bias.
- Without RSD, the main bias degeneracy limiting the experimental sensitivity is

$$P_{gg,\nabla^2\delta}(k) = -2 b_1 b_{\nabla^2\delta} \left(\frac{k}{k_*}\right)^2 P_{11}(k)$$

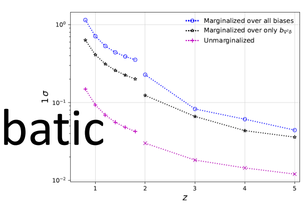

This is a feature of the **blue** isocurvature scenario that does not exist in the adiabatic case.

- Both the EFTofLSS sound speed and bias parameters receive novel UV sensitivity due to the blueness of the isocurvature spectrum.

Backup slides

Physics Reports 367 (2002) 1–248

SPT

$$\tilde{A}(\mathbf{k},\tau) = \int \frac{d^3\mathbf{x}}{(2\pi)^3} \exp(-i\mathbf{k}\cdot\mathbf{x}) A(\mathbf{x},\tau)$$

$$\tilde{\delta}(\mathbf{k},\tau) = \sum_{n-1} a^n(\tau)\delta_n(\mathbf{k})$$

$$\delta_n(\mathbf{k}) = \int d^3\mathbf{q}_1 \cdots \int d^3\mathbf{q}_n \, \delta_D(\mathbf{k} - \mathbf{q}_{1\cdots n}) F_n(\mathbf{q}_1,\ldots,\mathbf{q}_n)\delta_1(\mathbf{q}_1)\cdots\delta_1(\mathbf{q}_n)$$

$$\theta_n(\mathbf{k}) = \int d^3\mathbf{q}_1 \cdots \int d^3\mathbf{q}_n \, \delta_D(\mathbf{k} - \mathbf{q}_{1\cdots n}) G_n(\mathbf{q}_1,\ldots,\mathbf{q}_n)\delta_1(\mathbf{q}_1)\cdots\delta_1(\mathbf{q}_n)$$

$$\frac{\partial\tilde{\delta}(\mathbf{k},\tau)}{\partial\tau} + \tilde{\theta}(\mathbf{k},\tau) = -\int d^3\mathbf{k}_1\, d^3\mathbf{k}_2\, \delta_D(\mathbf{k}-\mathbf{k}_{12})\alpha(\mathbf{k}_1,\mathbf{k}_2)\tilde{\theta}(\mathbf{k}_1,\tau)\tilde{\delta}(\mathbf{k}_2,\tau),$$

$$\frac{\partial\tilde{\theta}(\mathbf{k},\tau)}{\partial\tau} + \mathscr{H}(\tau)\tilde{\theta}(\mathbf{k},\tau) + \frac{3}{2}\Omega_m\mathscr{H}^2(\tau)\tilde{\delta}(\mathbf{k},\tau) = -\int d^3\mathbf{k}_1\, d^3\mathbf{k}_2\, \delta_D(\mathbf{k}-\mathbf{k}_{12}) \times\beta(\mathbf{k}_1,\mathbf{k}_2)\tilde{\theta}(\mathbf{k}_1,\tau)\tilde{\theta}(\mathbf{k}_2,\tau)$$

$$F_2(\mathbf{q}_1,\mathbf{q}_2) = \frac{5}{7} + \frac{1}{2}\frac{\mathbf{q}_1\cdot\mathbf{q}_2}{q_1q_2}\left(\frac{q_1}{q_2}+\frac{q_2}{q_1}\right) + \frac{2}{7}\frac{(\mathbf{q}_1\cdot\mathbf{q}_2)^2}{q_1^2q_2^2}$$

$$G_2(\mathbf{q}_1,\mathbf{q}_2) = \frac{3}{7} + \frac{1}{2}\frac{\mathbf{q}_1\cdot\mathbf{q}_2}{q_1q_2}\left(\frac{q_1}{q_2}+\frac{q_2}{q_1}\right) + \frac{4}{7}\frac{(\mathbf{q}_1\cdot\mathbf{q}_2)^2}{q_1^2q_2^2}$$

$$F_n(\mathbf{q}_1,\ldots,\mathbf{q}_n) = \sum_{m=1}^{n-1}\frac{G_m(\mathbf{q}_1,\ldots,\mathbf{q}_m)}{(2n+3)(n-1)}[(2n+1)\alpha(\mathbf{k}_1,\mathbf{k}_2)F_{n-m}(\mathbf{q}_{m+1},\ldots,\mathbf{q}_n) + 2\beta(\mathbf{k}_1,\mathbf{k}_2)G_{n-m}(\mathbf{q}_{m+1},\ldots,\mathbf{q}_n)],$$

$$\alpha(\mathbf{k}_1,\mathbf{k}_2) \equiv \frac{\mathbf{k}_{12}\cdot\mathbf{k}_1}{k_1^2}$$

$$\beta(\mathbf{k}_1,\mathbf{k}_2) \equiv \frac{k_{12}^2(\mathbf{k}_1\cdot\mathbf{k}_2)}{2k_1^2k_2^2}$$

$$G_n(\mathbf{q}_1,\ldots,\mathbf{q}_n) = \sum_{m=1}^{n-1}\frac{G_m(\mathbf{q}_1,\ldots,\mathbf{q}_m)}{(2n+3)(n-1)}[3\alpha(\mathbf{k}_1,\mathbf{k}_2)F_{n-m}(\mathbf{q}_{m+1},\ldots,\mathbf{q}_n) + 2n\beta(\mathbf{k}_1,\mathbf{k}_2)G_{n-m}(\mathbf{q}_{m+1},\ldots,\mathbf{q}_n)]$$

$\mathbf{k}_1 \equiv \mathbf{q}_1 + \cdots + \mathbf{q}_m$, $\mathbf{k}_2 \equiv \mathbf{q}_{m+1} + \cdots + \mathbf{q}_n$, $\mathbf{k} \equiv \mathbf{k}_1 + \mathbf{k}_2$ and $F_1 = G_1 \equiv 1$

$$\Delta c^2_{\rm ren}(k_{\rm ren}, z) = c^2_{\rm ren,MX}(k_{\rm ren}, z) - c^2_{\rm ren,AD}(k_{\rm ren}, z)$$

$$c^2_{\rm ren,MX}(k_{\rm ren}, z) - c^2_{\rm ren,AD}(k_{\rm ren}, z) \approx \frac{P^{\rm AD}_{\rm 1-EFT}(k_{\rm ren}, z)}{P^{\rm AD}_{11}(k_{\rm ren}, z)} \times \frac{\alpha \left(\frac{f_c}{3}\right)^2 \left(\frac{T_{\rm iso}(k_{\rm ren})}{T_{\rm ad}(k_{\rm ren})}\right)^2 \left(\frac{k_{\rm ren}}{k_{\rm p}}\right)^{n_{\rm iso}-n_{\rm ad}}}{1 + \alpha \left(\frac{f_c}{3}\right)^2 \left(\frac{T_{\rm iso}(k_{\rm ren})}{T_{\rm ad}(k_{\rm ren})}\right)^2 \left(\frac{k_{\rm ren}}{k_{\rm p}}\right)^{n_{\rm iso}-n_{\rm ad}}} \times \left(0.284\, D(z)^{0.858} \alpha^{-0.147} \left(n_{\rm iso} - n_{\rm ad}\right) \left(\frac{k_s}{k_{\rm p}}\right)^{n_{\rm iso}-n_{\rm ad}}\right)$$

$$k_s \approx k_* \approx 0.2174 \ {\rm Mpc}^{-1}$$

$$k_{\rm p} = 0.05\,{\rm Mpc}^{-1}$$

Galaxies require baryons
Original EFTofLSS is about pressureless (before averaging) matter fluid

Consider matter dominated era when baryons are no longer coupled to the photons.

1412.5049

$$
\begin{aligned}
P^c(k) &= P^c_{11}(k) + P^A_{1-\mathrm{loop}}(k) - 2(2\pi)\left(\bar{c}^2_A(a_0) + w_b \bar{c}^2_I(a_0)\right) k^2 P^A_{11}(k) \\
P^b(k) &= P^b_{11}(k) + P^A_{1-\mathrm{loop}}(k) - 2(2\pi)\left(\bar{c}^2_A(a_0) - w_c \bar{c}^2_I(a_0)\right) k^2 P^A_{11}(k)
\end{aligned}
$$

$$
\begin{aligned}
P^A(k) &\equiv w_c^2 P^c + 2 w_c w_b P^{bc} + w_b^2 P^b \\
&= P^A_{11}(k) + P^A_{1-\mathrm{loop}}(k) - 2(2\pi)\bar{c}^2_A(a_0) k^2 P^A_{11}(k)
\end{aligned}
$$

On long wavelengths, the total matter can be well parameterized by pressureless matter fluid at 1-loop.

IR resummation

[1605.02149 (TSPT) , 2004.10607]

$$\Sigma^2(z) \equiv \frac{1}{6\pi^2}\int_0^{k_S} dq\, P_{\rm nw}(z,q)\left[1 - j_0\left(\frac{q}{k_{osc}}\right) + 2j_2\left(\frac{q}{k_{osc}}\right)\right]$$

$$P_{\rm mm,\,LO}(z,k) = P_{\rm nw}(z,k) + {\rm e}^{-k^2\Sigma^2(z)} P_{\rm w}(z,k)$$

$$P_{\rm tree,\,mm} = P_{\rm nw}(z,k) + {\rm e}^{-k^2\Sigma^2(z)} P_{\rm w}(z,k)(1 + k^2\Sigma^2(z))$$

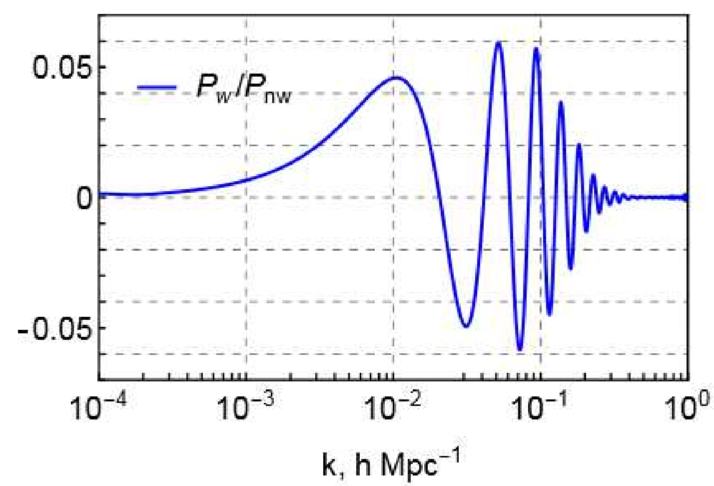

Built into CLASS-PT

Parameters: $\{n_{\rm iso}, \alpha\}$

$\{b_\epsilon^{[R]}, b_{\nabla^2\delta}^{[R]}, b_{\nabla^2\epsilon}^{[R]}\}$

Bias model for fiducial values:
[1201.3614, 1201.4827, 1812.03208]

$$b_2 = \frac{8}{21}(b_1 - 1), \qquad b_{\mathcal{G}_2} = -\frac{2}{7}(b_1 - 1), \qquad b_{\Gamma_3} = \frac{23}{42}(b_1 - 1)$$

$$b_\epsilon P_{\epsilon\epsilon} = P_{\rm shot} = 1/\bar{n}_g$$

Fiducial cosmology

$$A = 1 \qquad \Omega_b = 0.0486 \qquad \Omega_c = 0.2589 \qquad n_s = 0.9667 \qquad h = 0.6774$$

$$A_{\rm s,fid} = 2.1413 \times 10^{-9} \qquad A = A_{\rm s}/A_{\rm s,fid}$$

$$\sigma_{b_1} = 4, \quad \sigma_{b_2} = 2, \quad \sigma_{b_i} = 1$$

Error envelope corr length

$$k_{\rm p} = 0.05\,{\rm Mpc}^{-1} \qquad k_{\rm bin} = 0.01\,{\rm hMpc}^{-1} \qquad k_{\rm min} = 0.005\,{\rm hMpc}^{-1} \qquad \Delta k = 0.1\,{\rm hMpc}^{-1}$$

Blue isocurvature may be discoverable in the future

Thus far, there is no statistically significant blue isocurvature in data:

[1711.06736 /w Upadhye, 1807.06211]

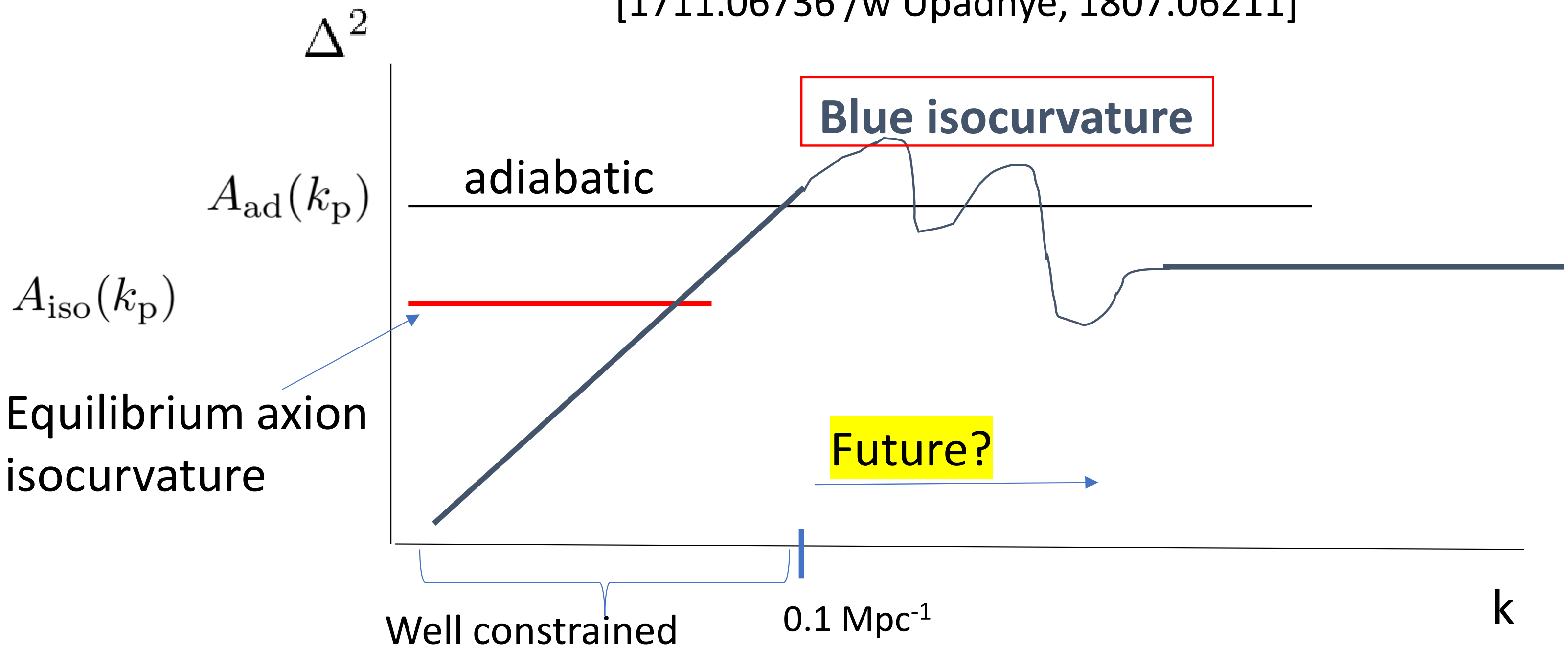

There is good prospects for seeing the break in future experiments.

$$\frac{k_\star}{a_0} \sim \left(\frac{\varphi_{\rm init}}{0.3M_p}\right)^{\frac{2}{3}} e^{-(N_e-50)} \left(\frac{T_{\rm rh}/H}{10^{-1}}\right)^{1/3} \left(\frac{H/\varphi_{\rm fin}}{10^{-3}}\right)^{2/3} (10\,{\rm Mpc}^{-1})$$

Large k information from data is important:

1) Blue isocurvature signal dominates at high k

$$\frac{k^3}{2\pi^2} P_{\mathcal{R}}(k) = A_{\rm ad}(k_{\rm p}) \left(\frac{k}{k_{\rm p}}\right)^{n_{\rm ad}-1}$$

$$\frac{k^3}{2\pi^2} P_{\mathcal{S}_{cdm}}(k) = A_{\rm iso}(k_{\rm p}) \left(\frac{k}{k_{\rm p}}\right)^{n_{\rm iso}-1}$$

$$\alpha = \frac{A_{\rm iso}(k_{\rm p})}{A_{\rm ad}(k_{\rm p})}$$

primordial

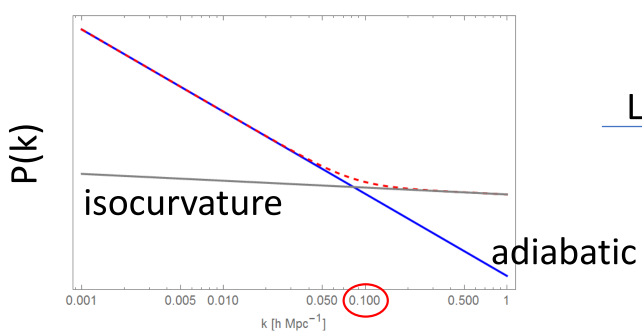

Linear evolve

Intuition

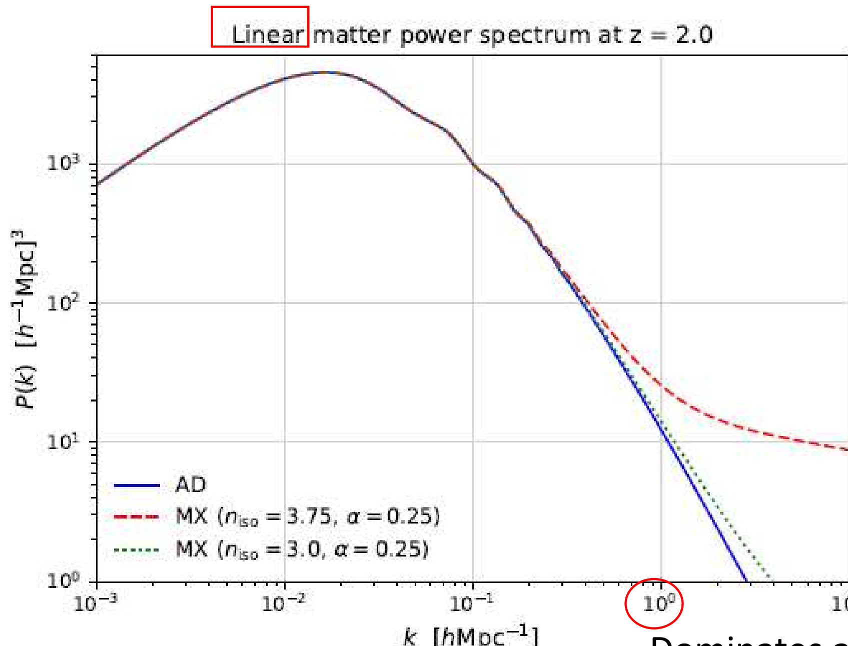

Dominates at later k

2) Phase space is large at high k (scales as k^3) → good possible source of information

EFTofLSS
[1004.2488, 1206.2926]

Idea: A) coarse grain the equation of motion → separates UV terms and IR terms
B) parameterize UV effective terms that can be matched to N-body simulations

EOM:

$$\nabla^2\phi - \frac{3}{2}\mathcal{H}^2\rho_0\delta = 0$$
$$\partial_\tau\delta + \nabla\cdot[(1+\delta)\,\vec{v}] = 0$$
$$\partial_\tau v + \mathcal{H}v + (v\cdot\nabla)\,v + \nabla\phi = 0$$

Separate UV and IR

Coarse grain over $1/\Lambda$ with a judicious window function:

$$W_\Lambda(\vec{x}-\vec{x}') = \left(\frac{\Lambda}{\sqrt{2\pi}}\right)^3 e^{-\frac{1}{2}\Lambda^2|\vec{x}-\vec{x}'|^2}$$

$$\delta_l(\vec{x}) \equiv [\delta(\vec{x})]_\Lambda \equiv \int d^3x' W_\Lambda(\vec{x},\vec{x}')\,\delta(\vec{x}')$$

$$\bar{v}_l(\vec{x}) = \frac{\int d^3x' W_\Lambda(\vec{x},\vec{x}')\,(1+\delta(\vec{x}'))\,\bar{v}(\vec{x}')}{1+\delta_l(\vec{x})}$$

[coarse grained velocity is a "composite" operator]

Key decoupling property: (sufficient locality and smoothness)

$$\int d^3x' W_\Lambda(\vec{x},\vec{x}')\,A_l(\vec{x}')B_s(\vec{x}') = -A_l(\vec{x})\frac{\nabla^2}{2\Lambda^2}B_l(\vec{x}) + O\left(\Lambda^{-4}\right)$$

long — short — Derivative expansion

$$A(\vec{x}) = A_l(\vec{x}) + A_s(\vec{x})$$

Effective Euler:

$$\rho_l(\vec{x})\left(\partial_\tau v_l(\vec{x}) + \mathcal{H}v_l(\vec{x}) + v_l^j(\vec{x})\partial_j v_l(\vec{x}) + \partial_i\phi_l(\vec{x})\right) \approx -\partial_j\left[\tau_i^j\right]_\Lambda$$

$$\left[\tau_i^j\right]_\Lambda = \left[\rho(\vec{x}')v_{si}(\vec{x}')v_s^j(\vec{x}') + \frac{2\partial^j\phi_s(\vec{x}')\partial_i\phi_s(\vec{x}') - \delta_i^j\partial^f\phi_s(\vec{x}')\partial_f\phi_s(\vec{x}')}{8\pi G}\right]_\Lambda$$

gravity — Coarse grain